Selective DNA Cleavage by Elsamicin A and Switch Function of Its Amino Sugar Group†

Motonari Uesugi, Takashi Sekida, Shinsuke Matsuki, and Yukio Sugiura*

Institute for Chemical Research, Kyoto University, Uji, Kyoto 611, Japan

Received January 16, 1991; Revised Manuscript Received April 17, 1991

ABSTRACT: We report guanine-specific recognition and selective cleavage of DNA by the antitumor antibiotic elsamicin A equipped with an amino sugar and compare these results with cleavage by chartarin and chartreusin antibiotics. The preferential cutting sites of DNA strand scission with elsamicin A are on the bases adjacent to the 3′-side of guanine residues such as 5′-GN sites, in particular 5′-GG sites. The present results also indicate that (1) the aglycon portion binds intercalatively to the 3′-side of guanine in host DNA, (2) the guanine 2-amino group has an important effect on selective DNA binding of elsamicin A, and (3) the amino sugar residue of elsamicin A facilitates the drug binding into the minor groove of B-DNA. In addition, we found that an acetylation of the amino group on the elsamicin A sugar portion plays an interesting switch function for the activity of elsamicin A. The biological implication of this switch has also been discussed.

There are a considerable number of DNA-binding antibiotics equipped with an amino sugar residue. The major questions to be asked about these antibiotics are, "To what sequence do the antibiotics bind?" and "What role do the amino sugar groups play?". With such questions in mind, our laboratory has studied the interaction of DNA and elsamicin A.

Elsamicin A is an antitumor antibiotic isolated from an actinomycete strain, J907-21, in El Salvador (Konishi et al., 1986). The antibiotic is structurally related to chartreusin containing the common aglycon, chartarin ring, but involves a different sugar moiety (Figure 1). The presence of the amino sugar group makes elsamicin A remarkably water-soluble and more bioactive than chartreusin (Sugawara et al., 1987), which was not developed clinically because of low solubility and rapid excretion into the bile (McGovren et al., 1977). Some attempts have been made to understand the key features responsible for antitumor activity of this family of antibiotics. Chartreusin inhibits biosynthesis of DNA as well as RNA and protein (Li et al., 1978), induces DNA strand scission in the presence of reducing agents (Yagi et al., 1981), and prevents negatively superhelical DNA from relaxation catalyzed by prokaryotic topoisomerase I (Uramoto et al., 1983). Therefore, the DNA molecule appears to be one of the important targets of these antibiotics.

In this work, we describe the experimental results designed (1) to explore the sequence specificity of the DNA–elsamicin A interaction and (2) to clarify the roles of the amino sugar group.

Experimental Procedures

Materials. Elsamicin A, chartreusin, and chartarin were kindly provided by Bristol-Meyers Squibb Research Institute (Tokyo, Japan). *N*-Acetylelsamicin A was obtained by reaction of elsamicin A with acetic anhydride and purified chromatographically (Sugawara et al., 1987). Plasmid pBR322 DNA was isolated from *Escherichia coli* C600. DNase I, *Sal*I, and *Dra*II were purchased from Takara Shuzo (Kyoto, Japan). All other chemicals used were of commercial reagent grade.

Preparation and Labeling of DNA Restriction Fragments. The restriction *Sal*I–*Dra*II fragment was labeled at the *Sal*I site. The 5′-end was labeled by using polynucleotide kinase and [γ-^{32}P]ATP, after treatment with bacterial alkaline phosphatase (Maxam & Gilbert, 1980). The 3′-end was labeled by using [α-^{32}P]dTTP and the *E. coli* DNA polymerase I large fragment. After digestion with the second enzyme, *Dra*II, the singly labeled fragment was purified by polyacrylamide gel electrophoresis.

Nucleotide Sequence Analysis. The reaction samples (total volume 20 μL) contained elsamicin A (10 μM), chartarin (20 μM), or chartreusin (20 μM) with the ^{32}P-end-labeled 128-bp (*Sal*I–*Dra*II) pBR322 DNA fragment, sonicated calf thymus carrier DNA (20 μg/mL), 20 mM Tris-HCl buffer (pH 7.5), and ferrous sulfate (10 μM for elsamicin A and 20 μM for chartreusin and chartarin). The cleavage reactions were initiated by addition of dithiothreitol (final concentration 1 mM), and allowed to proceed at 37 °C for 5, 20, and 10 min, respectively. To stop the reactions, Na_2EDTA (20 mM) and ice-cold ethanol were added to the samples. Each lyophilized sample was dissolved in 5 μL of loading buffer containing 5 M urea, 0.1% xylene cyanol FF, and 0.05 N NaOH and then heated at 90 °C before being loaded into a 10% polyacrylamide gel containing 7 M urea in 1× TBE buffer (1× TBE: 89 mM Tris–borate, 2 mM Na_2EDTA, pH 8). DNA sequencing was carried out by the Maxam–Gilbert method (Maxam & Gilbert, 1980). The autoradiograms were then scanned with a laser densitometer (LKB Model 2222 Ultro-Scan XL). In preparation of the histogram, a background cleavage was subtracted.

Pretreatments of DNA with Groove Binders. The aflatoxin B_1 modification of DNA (Suzuki et al, 1983) was carried out by addition of aflatoxin B_1 (100 μM, in CH_2Cl_2) and chloroperoxybenzoic acid (500 μM, in CH_2Cl_2) to the ^{32}P-end-labeled DNA preparation containing sonicated calf thymus DNA (20 μg/mL) in 20 mM Tris-HCl buffer (pH 7.5). After being shaken at 20 °C for 1 h, the aqueous layer was extracted with chloroform. In the competition experiment with distamycin A, the end-labeled DNA preparation was preincubated

† This study was supported in part by Grant-in-Aid for Scientific Research on Priority Area from the Ministry of Education, Science, and Culture, Japan.

0006-2960/91/0430-6711$02.50/0

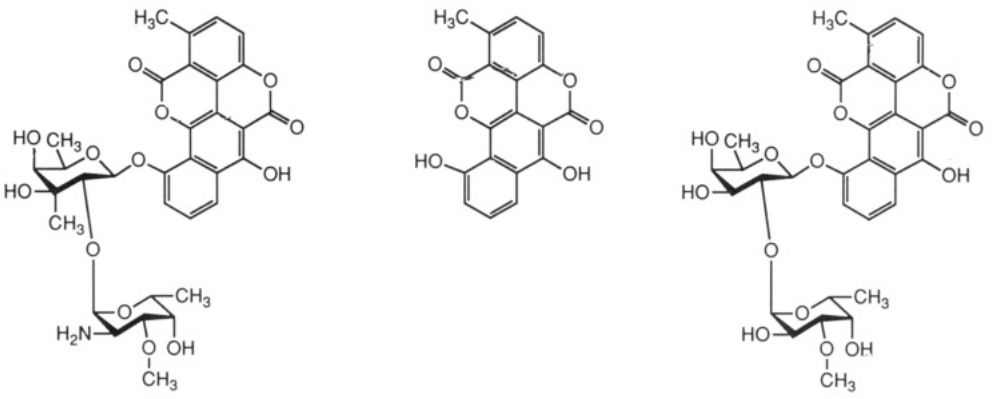

FIGURE 1: Chemical structures of elsamicin A, chartarin, and chartreusin.

with distamycin A (50 μM) in 20 mM Tris-HCl buffer (pH 7.5) at 37 °C for 30 min. The elsamicin A induced DNA cleavage of each sample was investigated and compared with the nucleotide sequence cleavage of intact DNA with elsamicin A.

DNase I Cleavage–Inhibition Analysis ("*Footprinting*"). The reaction mixtures contained the end-labeled DNA fragment, sonicated calf thymus DNA (5 μg/mL), and the drugs (15 or 30 μM) in 10 mM Tris-HCl (pH 7.5), 10 mM $MgCl_2$, and 5 mM $CaCl_2$. After preincubation at 37 °C for 30 min, the samples were digested with DNase I (final concentration 70 units/mL) for 1.5 min. The reactions were stopped by adding Na_2EDTA. After ethanol precipitation, the digestion products were resuspended in the loading buffer containing 5 M urea, 0.1% xylene cyanol FF, and 0.05 N NaOH. After boiling for 1 min, the samples were electrophoresed through a 10% polyacrylamide/7 M urea gel.

Assay for Damage to Supercoiled DNA. The reaction samples (total volume 20 μL) contained 0.8 μg of pBR322 plasmid DNA and elsamicin A (15 or 30 μM), *N*-acetylelsamicin A (15 or 30 μM), or chartreusin (15 or 30 μM) with 20 mM Tris-HCl buffer (pH 7.5) and ferrous sulfate (the equivalent concentrations as those of the drugs). The cleavage reaction was initiated by addition of dithiothreitol (1 mM). After incubation at 37 °C for 4 min, Na_2EDTA (20 mM) and ice-cold ethanol (70 μL) were added to stop the reaction. Each lyophilized sample was dissolved in 20 μL of loading buffer containing 0.05% bromophenol blue and 10% glycerol and then heated at 60 °C for 1 min before electrophoresis. Electrophoresis was performed by using a 1% agarose gel containing ethidium bromide (0.5 μg/mL) in 0.5 × TBE buffer.

Measurements of Fluorescence Spectra. Fluorescence emission spectra of the antibiotics and their DNA complexes were measured with a Hitachi F-3010 spectrofluorometer. The apparent binding constant between elsamicin A (or chartreusin) and poly[d(G-C)] was evaluated in 10 mM Tris-HCl buffer (pH 7.5) by a fluorescence-quenching method. The experimental data were analyzed by the neighbor-exclusion model of McGhee and von Hippel (1974), and the binding constant was obtained from the nonlinear least-squares fit.

ESR Measurements. The reaction mixture for spin trapping consisted of the 1:1 elsamicin A–Fe(II) complex (0.5–0.05 mM), dithiothreitol (1 mM), and *N-tert*-α-phenylnitrone (0.08 M; or 5,5-dimethyl-1-pyrroline *N*-oxide) in the buffered solution (pH 7.5). Oxygen was bubbled through the mixture, and then an aliquot of the sample solution was transferred to a quartz cell for ESR measurements (a JES-FE-3X spectrometer) at 25 °C. The ESR spectrum of the 1:1 elsamicin A–Fe(III) complex formed was detected at 77 K.

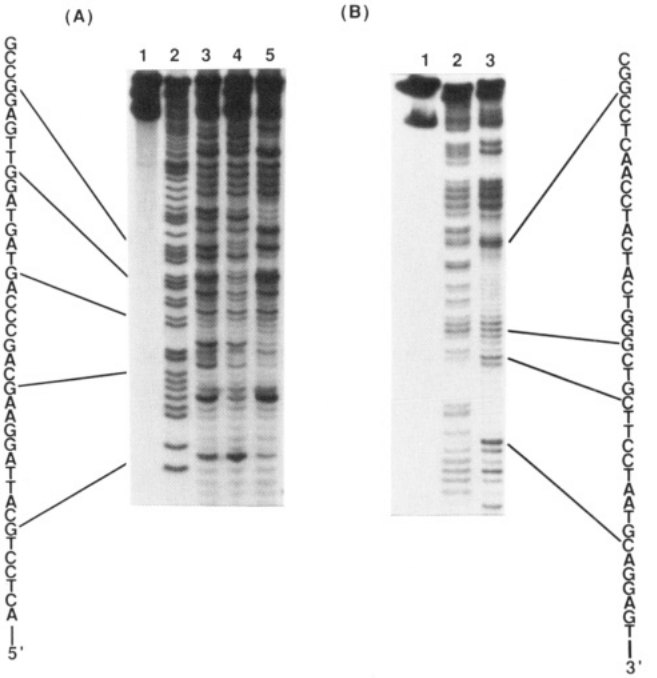

FIGURE 2: Autoradiograms of a 10% polyacrylamide/7 M urea slab gel electrophoresis for sequence analysis. (A) 5′-End-labeled pBR322 DNA (*Sal*I–*Dra*II fragment, 128 base pairs) was cleaved by elsamicin A (lane 3, 10 μM), chartarin (lane 4, 20 μM), and chartreusin (lane 5, 20 μM) in the presence of ferrous sulfate (10 μM for elsamicin A and 20 μM for chartarin and chartreusin) and dithiothreitol (1 mM) at pH 7.5. The reactions containing each drug were incubated at 37 °C for 5 min (lane 3), 20 min (lane 4), or 10 min (lane 5). (B) 3′-End-labeled DNA (the complementary strand of the same fragment) was cleaved by elsamicin A (lane 3, 10 μM) in the same way. Lane 1 in (A) and (B) shows intact DNA and lane 2 the Maxam–Gilbert sequencing for A+G.

RESULTS

Sequence Specificities of DNA Cutting. Figure 2A presents a typical autoradiographic result with the 5′-end-labeled 128-bp pBR322 DNA fragment on the DNA breakage by elsamicin A (lane 3), chartarin (lane 4), and chartreusin (lane 5) in the presence of ferrous sulfate and dithiothreitol. The three drugs show similar sequence-specific cutting modes. Cleavage data for the 3′-end-labeled strand of the same fragment by elsamicin A are also included in Figure 2B. These results clearly indicate that the cutting of double-stranded DNA by elsamicin A, chartreusin, and chartarin is specific at bases adjacent to the 3′-side of guanine (5′-GN sites) and

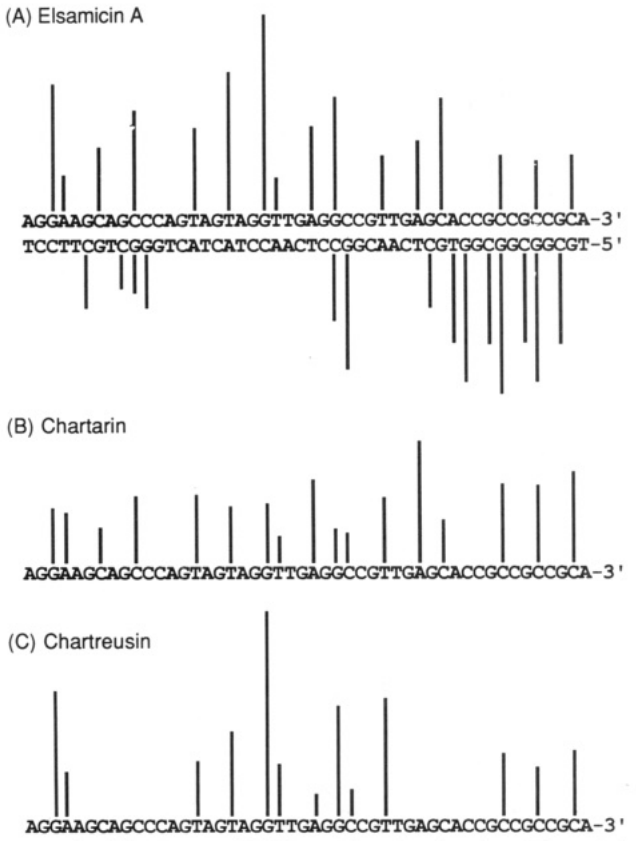

FIGURE 3: Histograms of DNA-cutting sites by elsamicin A (A), chartarin (B), and chartreusin (C). Relative DNA cleavage frequencies were obtained from densitometric scans of the gel autoradiograms shown in Figure 2. The heights of the bars present the relative cleavage intensities at the indicated base.

also is characteristic of single-strand scission. Figure 3 summarizes the DNA cleavage sites of elsamicin A, chartarin, and chartreusin. The sequence selective cleavage by the three compounds seems very similar but not identical. Particularly strong cleavage is observed at 5′-GG steps in elsamicin A and chartreusin. Under the same experimental conditions, the DNA cutting ability decreased in the order elsamicin A > chartreusin > chartarin.

Alterations of Elsamicin A Induced DNA Cleavage by Pretreatments of DNA with Groove Binders. Figure 4 demonstrates DNA strand scission generated by elsamicin A after pretreatment with distamycin A (lane 4) and aflatoxin B_1 (lane 5). These patterns were compared with the standard cleavage pattern for intact DNA (lane 3). Preincubation of the DNA fragment with distamycin A, which is a typical minor groove binder, strongly inhibited DNA strand scission by elsamicin A near A+T-rich regions. In contrast, covalent attachment of aflatoxin B_1 to the N-7 of guanine exhibited no obvious inhibitions of the elsamicin A induced DNA cleavage. It should be noted that the N-7 of guanine is situated in the major grooves of the DNA duplex.

DNA-Cleaving and -Binding Abilities of N-Acetylelsamicin A. To gain insight as to a significance of the amino sugar group, we investigated damages to supercoiled pBR322 DNA with elsamicin A, chartreusin, and *N*-acetylelsamicin A by using agarose gel electrophoresis. Their DNA breakages in the presence of ferrous sulfate and dithiothreitol are presented in Figure 5. The electrophoretic patterns for *N*-acetylelsamicin A (lanes 3 and 4) were almost identical with those for the controls with ferrous sulfate and dithiothreitol (lanes 7 and 8), whereas elsamicin A and chartreusin showed extensive fragmentation (lanes 1 and 2 for chartreusin; lanes 5 and 6 for elsamicin A). The results evidently showed that *N*-acetylelsamicin A is devoid of DNA cleavage activity, compared with elsamicin A and chartreusin. Further, we performed the DNase I cleavage–inhibition analysis for elsamicin A and *N*-acetylelsamicin A. Figure 6 presents a typical autoradiogram of the footprinting analysis. Comparison of DNase I digestion with (lanes 4 and 5) and without (lane 3) elsamicin A revealed several DNA footprints. In contrast, *N*-acetylelsamicin A (lanes 6 and 7) generated no obvious inhibition pattern for the digestion with DNase I.

Fluorescence Spectral Characteristics. When the excitation was at 266 nm, the fluorescence emission characteristics were

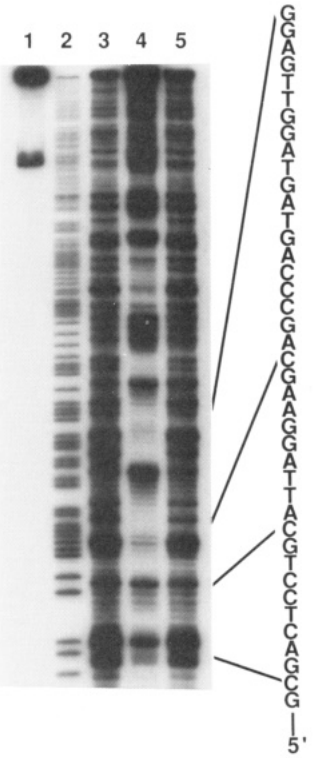

FIGURE 4: DNA-cutting modes with elsamicin A after pretreatment with distamycin A (lane 4) or aflatoxin B_1 (lane 5). After the pretreatment of the DNA fragment with the compounds, the DNA-cleavage reactions were carried out with elsamicin A (15 μM) in the presence of dithiothreitol (1 mM) and ferrous sulfate (15 μM) at 37 °C for 5 min. Lanes 1–3 show intact DNA alone, the Maxam–Gilbert sequencing reaction for A+G, and elsamicin A induced DNA cleavage for intact DNA, respectively.

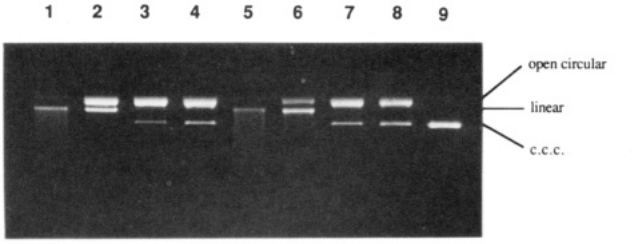

FIGURE 5: Agarose (1%) gel electrophoretic patterns of ethidium bromide stained pBR322 DNA after treatment with elsamicin A (lanes 5 and 6), *N*-acetylelsamicin A (lanes 3 and 4), and chartreusin (lanes 1 and 2). The samples contained 0.8 μg of pBR322 DNA, 20 mM Tris-HCl buffer (pH 7.5), ferrous sulfate (the equivalent concentrations to those of drugs), and the following additions: chartreusin (lane 1, 30 μM; lane 2, 15 μM), *N*-acetylelsamicin A (lane 3, 30 mM; lane 4, 15 μM), and elsamicin A (lane 5, 30 mM; lane 6, 15 μM). Lanes 7 and 8 show controls with ferrous sulfate (30 and 15 μM, respectively) in the absence of drugs, and lane 9 presents intact DNA alone. The reactions mixtures were incubated at 37 °C for 4 min in the presence of dithiothreitol (1 mM).

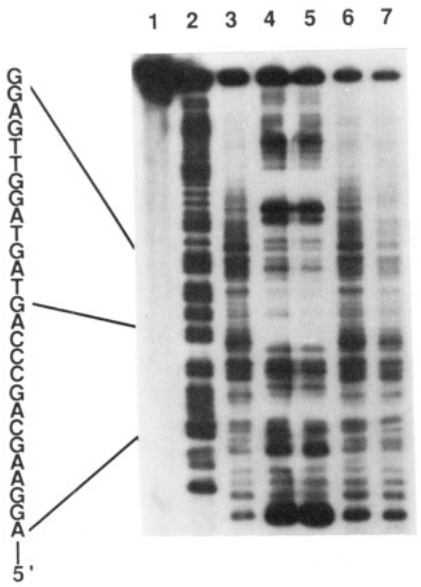

FIGURE 6: Autoradiograms of DNase I footprinting with elsamicin A and *N*-acetylelsamicin A. The DNA preincubated with elsamicin A (lane 4, 15 μM; lane 5, 30 μM) and *N*-acetylelsamicin A (lane 6, 15 μM; lane 7, 30 μM) and native DNA (lane 3) were digested with DNase I. Lane 2 shows the Maxam–Gilbert G+A sequencing reaction.

as follows: elsamicin A only, λ_{max} = 465 nm; elsamicin A plus poly[d(G-C)], 470 (sh) and 500 nm; elsamicin A plus poly[d(I-C)], 468 nm; elsamicin A plus poly[d(A-T)], 470 nm; and elsamicin A plus calf thymus DNA, 470 and 500 nm. In a similar fluorescence study of chartreusin, the shift with poly[d(G-C)] or calf thymus DNA was not observed, although the peak near 470 nm decreased with increasing concentration of DNA. The result suggests an important participation of guanine 2-amino and elsamicin A amino sugar groups for DNA–elsamicin A interaction. Indeed, apparent binding constants estimated by the fluorescence-quenching method were $(9.1 \pm 0.7) \times 10^4$ M^{-1} and $(3.4 \pm 0.1) \times 10^4$ M^{-1} for poly[d(G-C)] complexes of elsamicin A and chartreusin, respectively.

ESR Features of Elsamicin A–Iron Complex Systems. The ESR spin-trapping experiments presented the spin adducts of *N-tert*-α-phenylnitrone (triplet of doublet, g = 2.0057 and a^N = 15.3 G) and 5,5-dimethyl-1-pyrroline *N*-oxide (quartet, g = 2.0058 and $a^N = A_\beta^H$ = 15.2 G), evidently indicating the formation of hydroxyl radical in the elsamicin A–iron complex plus dithiothreitol system. The ESR signal (g = 4.4) of the 1:1 elsamicin A–Fe(III) complex was also characteristic of the non-heme-type high-spin ferric complex. In addition, the O-acetylation of the OH group of the chartarin core in elsamicin A lost both the iron complex formation and DNA cleavage activity. Therefore, the present site-specific DNA strand scission by elsamicin A may show that the production site of the active oxygen species is sterically near the base recognition of elsamicin A.

Discussion

Guanine-Specific Recognition and Minor Groove Interaction of Elsamicin A. Elsamicin A, chartarin, and chartreusin showed similar sequence-specific cutting modes, namely, 5′-GN site specificity, indicating that the aglycon portion of these antibiotics significantly contributes to the present selective recognition of the base sequence. While chartarin provides cleavage patterns similar to those of the glycons, it does not reveal DNA footprints under reaction with DNase I, suggesting that the sugar moieties have important binding activities but are not involved with strand damage. Fluorescence studies also point to a difference in binding between the glycons and the aglycon. Fluorescence spectral measurements clearly demonstrated that elsamicin A excludes the typical intercalator ethidium bromide from host DNA, and then the topoisomerase I unwinding assay (Pommier et al., 1987) indicated that elsamicin A positively winds relaxed closed circular duplex DNA (data not shown). These experimental results allow us to propose that the aglycon portion recognizes the guanine residue and binds intercalatively to the 3′-side of guanine in host DNA.

The covalent attachment of the guanine N-7 atom with aflatoxin B_1 gave no significant alterations for the nucleotide-specific cutting mode by elsamicin A. The fluorescence-quenching data revealed that the binding affinity of the antibiotic to T4 phage DNA is almost same as that to non-glucosylated mutant (T4dC) DNA. The former DNA is glucosylated at cytosine C-5 in the major groove. In contrast, distamycin A significantly altered the pattern of DNA cleavage by elsamicin A. Distamycin A is known to be a typical minor groove binder. The results highlight the interaction of elsamicin A in the minor groove of Watson–Crick double-helical DNA. Similarly, the nucleotide cleavage patterns generated by bleomycin (Kuwahara & Sugiura, 1988), esperamicin A_1 (Sugiura et al., 1989), and dynemicin A (Sugiura et al., 1990) are significantly affected by pretreatment of the DNA with distamycin A. These antibiotics are well-known to interact with the minor groove of the DNA helix. The aflatoxin B_1 pretreated and T4 phage DNAs would be expected to be less susceptible toward intercalation at GC pairs; namely, intercalation of the rather large chartarin ring should result in substantial steric interactions with these modified bases as it protrudes through the base stack into the major groove. This would be accentuated if the active species were the Fe(II) complex at the free phenolic hydroxyl. Therefore, it appears that DNA intercalation is one mode of binding and that DNA damage arises from a groove-bound complex. Indeed, the prototypical groove binder distamycin A caused substantial interference with DNA damage by elsamicin A.

Consistent with the above-mentioned results, elsamicin A inhibited DNA digestion with DNase I, which is established to interact with the minor groove of B-DNA. The inhibition analysis revealed certain binding sites such as 5′-GG and 5′-GC sequences for elsamicin A. On the other hand, chartarin gave no obvious inhibitions of the enzymatic cutting of DNA. The DNase cleavage–inhibition was clearly observed in the order of elsamicin A > chartreusin > chartarin. This observation underlines an importance of the sugar moiety for the stabilization of the DNA–elsamicin A complex, because the ability of any drug to induce a footprinting pattern depends on the strength of interaction and the slowness of drug–DNA dissociation (Low et al., 1984). Repeated experiments of the agarose gel electrophoreses also demonstrated that the DNA cleavage activity decreases in the order of elsamicin A > chartreusin > chartarin. These results add perspective on the features of DNA–elsamicin A encounter—the aglycon portion binds intercalatively to the 3′-side of guanine and the amino sugar residue is engulfed by the minor groove of host DNA. At the present stage, however, an intercalation to the 5′-side of guanine residues cannot be deleted completely.

It is also noteworthy that the preferred site of the elsamicin A mediated DNA degradation is significantly affected by the base adjacent to the 3′-side of guanine (5′-GG > 5′-GC, 5′-GT, 5′-GA). As shown in Figure 3, the cutting mode with chartarin considerably differs from those with elsamicin A and chartreusin, in which the best cleavages are consistently found at

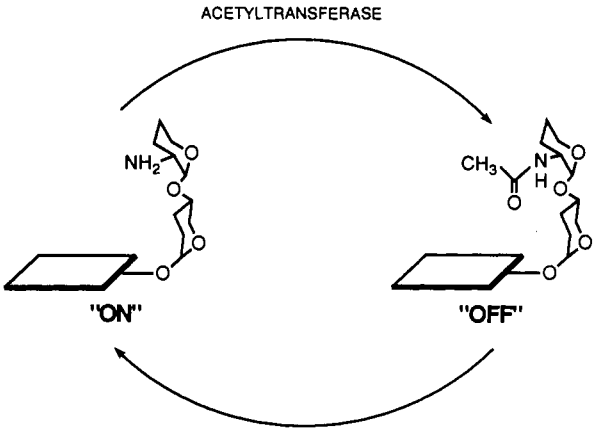

FIGURE 7: Schematic representation for the switch function of the amino sugar.

5′-GG sites. These observations lead us to postulate that the sugar residue interacts with 3′-side bases of guanine and that the GC pair–sugar complex is the most stable one. In addition, the fluorescence spectral data reveal that the 2-amino group of guanine residues and the amino sugar group of elsamicin A play an important role in DNA–elsamicin A interaction.

Switch Function of the Amino Sugar Group. N-Acetylation of the elsamicin A amino sugar group drastically inactivated the antibiotic not only in DNA cleavage activity but also in cytotoxicity and inhibitory activity on the biosynthesis of macromolecules such as DNA, RNA, and protein (Sugawara et al., unpublished data). The DNase I cleavage–inhibition analysis revealed that the remarkably low activity of *N*-acetylelsamicin A is due to the low binding affinity for DNA. In the ^{1}H NMR spectrum, the *N*-acetyl group (δ 0.80) of *N*-acetylelsamicin A resonates at unusually high magnetic field (Sugawara et al., 1987). Probably this is interpreted as a positional effect of the acetyl group over the chartarin ring. These results suggest that the poor DNA binding of the *N*-acetyl derivative is due to a steric effect rather than a charge neutralization effect. Namely, the acetylation of the amino sugar moiety in elsamicin A sterically hinders the antibiotic from intercalation to DNA.

The present finding suggests that the amino sugar residue functions as a biological switch—the amino sugar group may be capable of controlling the activity of the DNA-binding molecule especially in resistant strains and the producing strain (Figure 7). Similar mechanisms of resistance have been found in aminoglycoside antibiotics such as kanamycins, gentamicins, and neomycins, which are well-known to be enzymatically inactivated by acetylation of the amino sugar (Benveniste & Davies, 1973). It has also been demonstrated that the N-acetylation of daunomycin markedly lowers both DNA-binding affinity and biological activity (Di Marco & Arcomone, 1975). Therefore, the switch function of the amino sugar residue may be one key regulatory action in antitumor anthracycline glycosides. This paper focuses on guanine-specific recognition and the roles of the amino sugar group of elsamicin A. Further studies of this type are likely to lead to a more rational drug design and better strategies in cancer chemotherapy.

References

Benveniste, R., & Davies, J. (1973) *Annu. Rev. Biochem. 42*, 471–506.

Di Marco, A., & Arcomone, F. (1975) *Arzneim.-Forsch. 25*, 368–375.

Konishi, M., Sugawara, K., Kofu, F., Tomita, K., Miyaki, T., & Kawaguchi, H. (1986) *J. Antibiot. 39*, 784–791.

Kuwahara, J., & Sugiura, Y. (1988) *Proc. Natl. Acad. Sci. U.S.A. 85*, 2459–2463.

Li, L. H., Clark, T. D., Murch, L. L., Wooden, J. M., Pschigoda, L. M., & Krueger, W. C. (1978) *Cancer Res. 38*, 3012–3018.

Low, C. M. L., Drew, H. R., & Waring, M. J. (1984) *Nucleic Acids Res. 12*, 4865–4879.

Maxam, A. M., & Gilbert, W. (1980) *Methods Enzymol. 65*, 449–560.

McGhee, J. D., & von Hippel, P. H. (1974) *J. Mol. Biol. 86*, 469–489.

McGovren, J. P., Neil, G. L., Crampton, S. L., Robinson, M. I., & Douros, J. D. (1977) *Cancer Res. 37*, 1666–1672.

Pommier, Y., Covey, J. M., Kerrigan, D., Markovits, J., & Pham, R. (1987) *Nucleic Acids Res. 16*, 6713–6731.

Sugawara, K., Tsunakawa, M., Konishi, M., & Kawaguchi, H. (1987) *J. Org. Chem. 52*, 996–1001.

Sugiura, Y., Uesawa, Y., Takahashi, Y., Kuwahara, J., Golik, J., & Doyle, T. W. (1989) *Proc. Natl. Acad. Sci. U.S.A. 86*, 7672–7676.

Sugiura, Y., Shiraki, T., Konishi, M., & Oki, T. (1990) *Proc. Natl. Acad. Sci. U.S.A. 87*, 3831–3835.

Suzuki, T., Kuwahara, J., & Sugiura, Y. (1983) *Biochem. Biophys. Res. Commun. 117*, 916–922.

Uramoto, M., Kusano, T., Nishino, T., Isono, K., Shishido, K., & Ando, T. (1983) *FEBS Lett. 153*, 325–328.

Yagi, M., Nishimura, T., Suzuki, H., & Tanaka, H. (1981) *Biochem. Biophys. Res. Commun. 98*, 642–647.